

Active-gel Theory for Multicellular Migration of Polar Cells in the Extra-cellular Matrix

Ram M. Adar^{1,2,3} and Jean-François Joanny^{1,2,3}

¹ Collège de France, 11 place Marcelin Berthelot, 75005 Paris, France

² Laboratoire Physico-Chimie Curie, Institut Curie, Centre de Recherche, Paris Sciences et Lettres Research University, Centre National de la Recherche Scientifique, 75005 Paris, France

³ Université Pierre et Marie Curie, Sorbonne Universités, 75248 Paris, France

Abstract. We formulate an active-gel theory for multicellular migration in the extra-cellular matrix (ECM). The cells are modeled as an active, polar solvent, and the ECM as a viscoelastic solid. Our theory enables to analyze the dynamic reciprocity between the migrating cells and their environment in terms of distinct relative forces and alignment mechanisms. We analyze the linear stability of polar cells migrating homogeneously in the ECM. Our theory predicts that, as a consequence of cell-matrix alignment, contractile cells migrate homogeneously for small wave vectors, while sufficiently extensile cells migrate in domains. Homogeneous cell migration of both extensile and contractile cells may be unstable for larger wave vectors, due to active forces and the alignment of cells with their concentration gradient. These mechanisms are stabilized by cellular alignment to the migration flow and matrix stiffness. They are expected to be suppressed entirely for rigid matrices with elastic moduli of order 10 kPa. Our theory should be useful in analyzing multicellular migration and ECM patterning at the mesoscopic scale.

1. Introduction

Multicellular migration plays a key role during development, wound healing and metastasis [1, 2, 3]. A basic distinction can be made between solid-like and fluid-like migration, which differ in the strength and duration of cell-cell adhesions. Fluid-like migration is referred to as “multicellular streaming” [4, 5] and is the main motivation for this paper. The migration mode depends on the properties of the cells and their environment. Polarization is important for cell migration in both the single-cell and multicellular levels. Intuitively, cells with a well-defined direction migrate in this direction. The constant crosstalk between migrating cells and their environment is also gaining increasing attention as an essential factor for multicellular migration [5, 6, 7, 8]. This is referred to as “dynamic reciprocity” [7] or “mechanoreciprocity” [8].

We focus on migration that takes place in the extra-cellular matrix (ECM), which consists mostly of collagen I. It was shown that anisotropic ECM organization with aligned collagen fibres promote cancer-cell migration in collagen tracks [5, 9]. Cells are able to remodel the fibres and change their environment, either mechanically or chemically. For example, interactions between ECM fibers and fibroblasts tune ECM properties and can account for variations in matrix isotropy, density, and homogeneity found across different tissues [10]. The viscoelastic nature of the matrix is also important in tumor growth and cancer-cell invasion [11]. For example, collagen relaxation was shown to drive the motion of cancer-cell clusters on collagen gels in two dimensions [12].

While several mathematical models have been proposed for multicellular migration in the ECM in different contexts [13, 14, 15, 16, 17, 18], a physical understanding of cell-ECM interaction at the mesoscopic scale and in three dimensions is still missing. Here, we propose to describe the ECM together with the migrating cells as an active, permeating, polar gel. Such systems were studied in the past in different contexts [19, 20, 21, 22, 23, 24, 25]. We rely mostly on our recent work [25], which explored permeation instabilities of an active, polar, solvent immersed in a viscoelastic fluid. This theory was formulated as a two-fluid model, with a clear distinction between forces that act on the network and solvent separately and relative forces between them.

In this work, we develop our theory further and adapt it to cells in the ECM. We formulate a solid-fluid model, considering that the ECM is solid at long times, and take into account cell division and strain-polarization alignment. We analyze the linear stability of a homogeneous flow of polarized cells. Instabilities infer transient and possibly long-lived, migrating cell collections.

Our key findings are: 1) Cell-matrix interactions can be classified according to their characteristic spatial order, dynamics, activity, reversibility, and elasticity. 2) Active stresses can destabilize flexible matrices. 3) Matrix stiffness stabilizes the ECM and suppresses alignment-driven instabilities. 4) ECM stability for small wave vectors is determined by the active nematic stress; it is stable for contractile cells and unstable for sufficiently extensile cells. 5) Alignment of polarization to concentration gradients can either stabilize or destabilize the ECM, while alignment to the migration current

stabilizes it. The former can change the transient domain size by orders of magnitude.

The outline of the paper is as follows: In Sec. 2, we derive our theory for multicellular migration in the ECM, in terms of an active, polar fluid permeating in a viscoelastic solid. Next, we highlight in Sec. 3 the different matrix-cell interactions that arise naturally from our theory. In Sec. 4 we derive the linearized equations that determine the linear stability of the system. The analysis is performed in the isotropic case and in the rigid-matrix limit in Secs. 5 and 6, respectively. We analyze the stability in the general case in Sec. 7 and clarify the stabilizing or destabilizing role of cell-matrix alignment mechanisms. We conclude in Sec. 8 by discussing possible extensions of our theory and how it relates to biologically-relevant scenarios.

2. Theory

We consider a two-component gel, composed of active, polar cells (c) and a viscoelastic matrix (m). The polarization field is given by the unit vector \mathbf{p} . The matrix is modeled as a viscoelastic solid; fluid at short times and solid at long times. Its deviation from the reference state is given by the displacement vector \mathbf{u} . The matrix has a volume fraction ϕ , and the cells $1 - \phi$. The gel is assumed to be incompressible.

The free energy of the gel can be written as

$$F = \int d^3r \left[k_B T a^{-3} (1 - \phi) \ln(1 - \phi) + \phi (1 - \phi) [\chi_0 + \psi \text{Tr}(\mathbf{Q}\boldsymbol{\epsilon})] + \kappa (\nabla\phi)^2 + K \left(\frac{1}{2} (\nabla\mathbf{p})^2 - l_p^{-1} \mathbf{p} \cdot \nabla\phi \right) - \frac{1}{2} h_{\parallel} \mathbf{p}^2 + \frac{\phi}{\phi_0} \left(G \text{Tr}(\tilde{\boldsymbol{\epsilon}}^2) + \frac{1}{2} B \epsilon^2 \right) \right]. \quad (1)$$

The first line is the Flory-Huggins free energy of a binary mixture in the limit long polymer chains, where $k_B T$ is the thermal energy and a is a microscopic length. The χ_0 term accounts for short-range interactions, and ψ to an aligning interaction (see, e.g., [24, 26, 27, 28]) that is related to three-dimensional ‘‘contact guidance’’ in biological contexts. It is written in terms of the nematic tensor $Q_{\alpha\beta} = p_{\alpha}p_{\beta} - 1/3 \delta_{\alpha\beta}$ and linearized strain tensor $\epsilon_{\alpha\beta} = (\partial_{\alpha}u_{\beta} + \partial_{\beta}u_{\alpha})/2$. It results in a shear elastic stress in the reference state, which aligns the matrix parallel or normal to the polarization axis ($\psi < 0$ or $\psi > 0$, respectively). The κ term accounts for the interfacial tension that suppresses large concentration gradients.

The first part of the second line accounts for variations of the polarization field from the homogeneously polarized state [29, 30], where K is the Frank constant in the one-constant approximation. It is generally a function of the cellular volume fraction, but this dependence does not play any role in our linear analysis and is disregarded hereafter. The second term accounts for alignment with respect to concentration gradients in terms of the length l_p . This describes, for example, cellular alignment at cluster interfaces, similarly to anchoring at droplet interfaces [31]. We refer hereafter to this mechanism as ‘‘concentration alignment’’. The h_{\parallel} term is a Lagrange multiplier to ensure that $\mathbf{p}^2 = 1$.

The final contribution is the elastic free energy. For simplicity, we restrict ourselves to linear elasticity, where G and B are the shear and bulk moduli for $\phi = \phi_0$,

respectively. We decompose the strain into the scalar $\epsilon = \epsilon_{\alpha\alpha}$ and the traceless tensor, $\tilde{\epsilon}_{\alpha\beta} = \epsilon_{\alpha\beta} - \epsilon/3 \delta_{\alpha\beta}$.

We describe the dynamics of the concentration, polarization, and displacement fields within a thermodynamic framework. The matrix moves with a velocity $\mathbf{v}^m = \partial \mathbf{u} / \partial t$ and the cells with a velocity \mathbf{v}^c , corresponding to a center-of-mass (COM) velocity, $\mathbf{v} = \phi \mathbf{v}^m + (1 - \phi) \mathbf{v}^c$, and a relative current, $\mathbf{j} = \phi(1 - \phi)(\mathbf{v}^m - \mathbf{v}^c)$. We assume the same specific mass for both components.

Living cells are active. They are constantly driven out of equilibrium by the input of an energy $\Delta\mu$ that corresponds, for example, to the chemical potential difference between ATP and its hydrolysis products [32, 19]. In particular, the cells divide and die, while the mass of the matrix is conserved, i.e.,

$$\partial_t \phi + \nabla \cdot (\phi \mathbf{v}^m) = 0, \quad \partial_t (1 - \phi) + \nabla \cdot [(1 - \phi) \mathbf{v}^c] = (1 - \phi) k \approx k_\phi (\phi - \phi_0). \quad (2)$$

The cellular growth rate, k , is generally a function of the pressure [33, 34]. We linearize the right hand side around the homeostatic pressure and volume fraction ϕ_0 , where cell division and death balance each other, in terms of the rate $k_\phi > 0$. In Eq. (2), cell division and death are related only to cell component. A more detailed description would include a third solvent component that exchanges mass with the cells as part of these processes. Coarse-graining over the solvent neglects cell-solvent friction. This is reasonable because the cells are much more viscous than the solvent, making cell-matrix friction more important. This description also neglects active matrix deposition and degradation by the cells, which can be especially important for fibroblasts. The study of this effect is reserved for future work. Note that the incompressibility condition is affected by the active growth rate and is given by $\nabla \cdot \mathbf{v} = k_\phi (\phi - \phi_0)$.

For the polarization, we derive in Appendix A the following constitutive relation:

$$(\partial_t + \mathbf{v}^c \cdot \nabla) \mathbf{p} = \bar{h}_\parallel \mathbf{p} + \mathbf{p} \cdot \nabla \mathbf{v}^c + D_p \nabla^2 \mathbf{p} + D_p l_p^{-1} \nabla \phi + \lambda \mathbf{j} + \phi(1 - \phi) \bar{\psi} \boldsymbol{\epsilon} \cdot \mathbf{p}. \quad (3)$$

The first term on the right-hand side originates from h_\parallel of Eq. (1) and ensures that $\mathbf{p}^2 = 1$. The next term accounts for the shear alignment of the cells as if they were solid rods (shear-alignment parameter of -1) and $D_p = K/\gamma_1$ is the angular diffusion constant, with γ_1 the rotational viscosity. The final three terms in Eq. (3) describe polarization alignment due to cell-matrix interaction. The first describes alignment to concentration gradients, while λ is the permeation-alignment constant [25] that describes how the cells align to their migration current in the matrix. Finally, $\bar{\psi}$ describes cell-matrix alignment due to the ψ term in Eq. (1) and possible active mechanisms. We focus on passive alignment, for which $\bar{\psi} = -2\psi/\gamma_1$ (see Appendix A). These alignment mechanisms are illustrated in Fig. 1.

Equations (2) and (3) describe the dynamics of the cell concentration and orientation. They depend on the cell velocity and matrix displacement, which can be determined from force balance equations. We make use of a solid-fluid model, similar to the fluid-fluid model of Ref. [25]. Force-balance equations are written separately for the matrix and cells as

$$\mathbf{f}^m - \phi \nabla \delta P = \mathbf{f}^{\text{rel}}, \quad \mathbf{f}^c - (1 - \phi) \nabla \delta P = -\mathbf{f}^{\text{rel}}, \quad (4)$$

where \mathbf{f}^m and \mathbf{f}^c are the forces acting on the matrix and cells, respectively, δP is a pressure difference that enforces global incompressibility, and \mathbf{f}^{rel} is the relative force between the two components.

The forces acting on each of the components are

$$\mathbf{f}_\alpha^m = \partial_\beta \left[\sigma_{\alpha\beta}^{\text{el}} + \frac{\phi}{\phi_0} (2G\tau\partial_t\tilde{\epsilon}_{\alpha\beta} + B\bar{\tau}\partial_t\epsilon\delta_{\alpha\beta}) \right] - \phi\partial_\alpha\bar{\mu}, \quad (5)$$

$$\mathbf{f}_\alpha^c = \partial_\beta \left[-h_\alpha p_\beta + (1 - \phi) (\bar{\zeta}\delta_{\alpha\beta} + \zeta Q_{\alpha\beta}) \right] - h_\beta\partial_\alpha p_\beta, \quad (6)$$

where the summation convention was used. Here, $\sigma_{\alpha\beta}^{\text{el}} = \delta F/\delta\epsilon_{\alpha\beta}$ is the elastic stress and the next two terms describe the viscoelastic shear and compressional stresses, in terms of the shear and compressional retardation times, τ and $\bar{\tau}$, respectively. The last term is the osmotic pressure gradient, with the relative chemical potential $\bar{\mu} = \delta F/\delta\phi$.

In Eq. (6), the first term is the stress due to shear alignment, where $\mathbf{h} = -\delta F/\delta\mathbf{p}$ is the orientational field. Next is the active cellular stress that consists of an isotropic contribution $\sim \bar{\zeta}$ and a traceless contribution $\sim \zeta$, proportional to the nematic tensor, \mathbf{Q} . The stresses $\bar{\zeta}$ and ζ are considered as constants, neglecting the possible dependence on matrix properties [35]. The last term in Eq. (6) originates in the Ericksen stress and vanishes to linear order around a polarized state. The cellular viscous dissipation has been neglected; it is negligible compared to the relative friction force on lengthscales larger than the matrix mesh size, which are relevant to our hydrodynamic framework.

The cell-matrix relative force is given by

$$\mathbf{f}^{\text{rel}} = \frac{1}{\gamma}\mathbf{j} - \phi(1 - \phi)(\lambda\mathbf{h} + \nu\mathbf{p} + \nu'\boldsymbol{\epsilon} \cdot \mathbf{p}). \quad (7)$$

The first term is the friction force, where γ is the mobility. The term $\sim \lambda$ is the reactive force associated with permeation alignment [25]. The last two terms are active forces that are the main contributors to cell motility in the polar case. The ν' term can also be related to anisotropic friction due to matrix strain, as is explained in Appendix B.

3. Description of cell-matrix interaction

Our framework is convenient for analyzing the crosstalk between cells and their environment and classifying its underlying mechanisms. First, the matrix and cells influence each other indirectly, because they are constrained by global force balance [sum of the two lines in Eq. (4)]. At the same time, each component undergoes convection according to its own velocity, which is also determined from the force-balance equations. More interestingly, we can identify and classify mechanisms of direct interaction between the cells and the matrix. These include the friction force and active relative forces, as well as permeation alignment, concentration alignment, and strain-polarization alignment. The three alignment mechanisms are illustrated in Fig. 1.

The interaction terms require a combination of matrix and cells and vanish in pure phases ($\phi = 0, 1$). They are especially important in the case of multicellular streaming and small matrix mesh size, where cells can flow and mix with the matrix on a mesoscopic

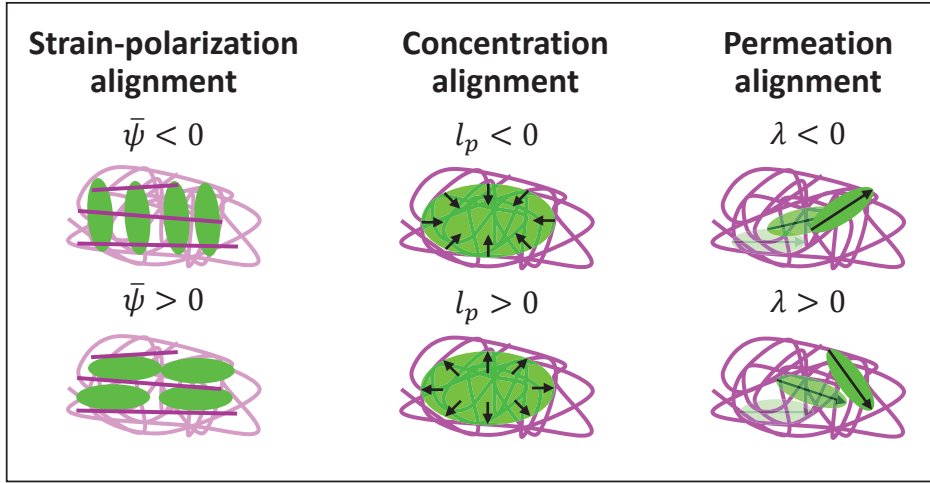


Figure 1: (Color online) Heuristic description of alignment mechanisms of polar cells (green, polarization indicated by a black arrow) in a viscoelastic matrix (purple). The strain-polarization term aligns the matrix segments normal or parallel to the polarization axis ($\bar{\psi} < 0$ or $\bar{\psi} > 0$, respectively). The concentration-alignment term aligns the polarization towards or away from gradients in cell concentration ($l_p < 0$ or $l_p > 0$, respectively). The permeation-alignment term aligns the cell towards or away from its direction of relative motion ($\lambda < 0$ or $\lambda > 0$, respectively).

scale. This mixing yields bulk interaction terms and relative forces that exist between the cells and matrix within each volume element, rather than surface terms that exist only between clearly separated phases.

Table 1: Classification of cell-matrix interaction terms.

Mechanism	Dynamics	Reversibility	Activity	Symmetry	Elasticity
Friction	dynamic	dissipative	passive	isotropic	none
Active relative force	dynamic	reactive	active	polar	none/elastic
Permeation alignment	dynamic	reactive	passive	polar	none
Concentration alignment	static	dissipative	passive	polar	none
Strain-polarization alignment	static	dissipative	passive / active	nematic	elastic

The thermodynamic framework allows to classify these mechanisms according to five categories (and see Table 1); *Dynamics* - requires cell migration (dynamic) or not (static). *Reversibility* - produces entropy (dissipative) or not (reactive). *Activity* - requires ATP hydrolysis (active) or not (passive). *Symmetry* - requires polar order, nematic order, or no order (isotropic). *Elasticity* - requires elasticity or not. As is evident from Table 1, each mechanism is unique according to this classification. This demonstrates that the different terms of our theory have distinguishable properties and can be inferred from sufficient experimental data.

4. Linear stability analysis

The system has a homogeneous steady state at the homeostatic concentration $\phi = \phi_0$ and is in a fully polarized state that we set as $\mathbf{p}^0 = \hat{\mathbf{x}}$. The active relative force drives a homogeneous steady-state current $\mathbf{j}^0 = j_0 \mathbf{p}^0$ (see Appendix B). This effect is purely active and polar. As the concentration and polarization are homogeneous, the active cellular stress and matrix alignment stress are constant, and the matrix displacement is determined by the boundary conditions. We consider the case where the matrix is in its equilibrium configuration, meaning that the stress on the boundaries matches the active stress. The steady-state strain is then given by $\boldsymbol{\epsilon} = -\psi \phi_0 (1 - \phi_0) \mathbf{Q}/2G$. As cells are mostly known to align parallel to matrix segments, the sign $\psi < 0$ is chosen.

We analyze the linear stability of the steady state with respect to perturbations with a growth rate s and wave vector q , of the form $\mathbf{x} = \mathbf{x}^0 + \mathbf{x}^1 \exp(st + i\mathbf{q} \cdot \mathbf{r})$, where $\mathbf{x} = (\phi, \mathbf{p}, \mathbf{u})$. For simplicity, we focus on wave vectors perpendicular to the steady-state polarization, $q_x = 0$, assuming that heterogeneity is most notable normal to the direction of migration. As the matrix is elastic, its concentration changes only via strain, according to $\phi^1/\phi_0 = -\epsilon^1$. This relates the normal components of the displacement, u_y^1 and u_z^1 to ϕ^1 . In addition, ϕ^1 is affected only by the divergence of the polarization, $i\mathbf{q} \cdot \mathbf{p}^1 \equiv p_d^1$. This is reasonable because, around the polarized state and to linear order, this is the only scalar obtained from \mathbf{p}^1 . These arguments reduce the dimensions of the linear stability analysis to three, corresponding to ϕ^1 , p_d^1 , and u_x^1 .

We find u_x^1 as a function of the concentration and polarization and obtain the following linearized equations (see Appendix B):

$$s\phi^1 = - [k_\phi + (D_\phi + l_\eta^2 s) q^2] \phi^1 - [j_0 + j_u u_p + D_p (l_p^{-1} - \lambda) l_{\gamma_1}^2 q^2] p_d^1, \quad (8)$$

$$s p_d^1 = - [(\bar{\psi} - \lambda j_u) u_p + D_p (1 + \lambda (\lambda - l_p^{-1}) l_{\gamma_1}^2) q^2] p_d^1 + [\lambda (D_\phi + l_\eta^2 s) - l_p^{-1} D_p] q^2 \phi^1. \quad (9)$$

The parameters that appear in Eqs. (8) and (9) are listed in Table 2. In Eq. (8), the first term describes the concentration relaxation due to active cell division and death. The terms quadratic in q account for osmotic diffusion, where D_ϕ is the effective diffusion coefficient in the presence of elasticity, permeation alignment and active cellular stress. $l_\eta = \sqrt{(1 - \phi_0) \gamma (4G\tau/3 + B\bar{\tau})/\phi_0}$ is a screening length that arises from the interplay between transient matrix viscosity and cell-matrix friction.

The second part of Eq. (8) accounts for the relative force in the direction of \mathbf{p}^1 . The first two terms relate to the active relative current. j_0 is the steady-state current, while $j_u = \gamma (2\lambda\phi_0 (1 - \phi_0) \psi - \nu')$ describes a correction due to the network strain. The term u_p is a function of the rate τs and is related to the network displacement in the x -direction, due to strain-polarization coupling (see Sec. 6 and Appendix B). The relative force quadratic in q originates from concentration-polarization alignment, with $l_{\gamma_1} = \sqrt{\phi_0 (1 - \phi_0) \gamma \gamma_1}$ being a screening length due to the interplay between rotational viscosity and friction.

In Eq. (9), the first term describes a q^0 polarization rate resulting from network-

strain coupling (see Sec. 7.1). The term quadratic in q is the effective angular diffusion constant. Alignment to concentration gradients and flow may render it negative. The second line of Eq. (9) describes the two mechanisms of polarization rotation due to concentration gradients; one is dynamic (permeation alignment $\sim \lambda$) and the second is static (concentration alignment $\sim l_p^{-1}$). The two mechanisms either add up or compete with each other.

This linear set of equation can be written as $M \cdot \mathbf{x} = 0$, where $\mathbf{x} = (\phi^1, p_d^1)^T$. The dispersion relation $s(q)$ is found by solving $\det M = 0$. The system is stable if $\text{Re } s < 0$ for all the eigenvalues of the linear system. The stability analysis is involved, due to the large number of mechanisms that take place. Therefore, we focus first on two limiting cases of isotropic cells and a rigid matrix. Then, we analyze separately the different alignment mechanisms and their effect on stability.

Table 2: Parameters of the theory. Estimations of the parameters are found in Appendix D.

Symbol	Description	Symbol	Description
D_ϕ	effective osmotic diffusion constant	l_ϕ	interfacial correlation length
k_ϕ	cellular division rate	D_p	angular diffusion constant
l_η	screening length due to matrix viscosity	$l_{\gamma 1}$	screening length due to rotational viscosity
ψ	strain-polarization alignment rate	u_p	measure of polarization-induced network x -displacement
j_0	steady-state relative current	j_u	$j_u u_p$ is the strain-induced relative current
l_p	concentration-alignment coupling (length)	λ	permeation-alignment coupling (inverse length)

5. Isotropic case: active stresses may destabilize a flexible ECM.

Cells are in many cases isotropic. The polarization terms then drop out of the equations, and the dispersion relation is found from Eq. (8) as $s = -(k_\phi + D_\phi q^2) / (1 + l_\eta^2 q^2)$. This situation was explored by Murray, Oster, and Harris [13, 14] in their works on mesenchymal morphogenesis, which similarly describe cell migration as fluid flow in a viscoelastic solid.

The stability is determined by the sign of the osmotic diffusion constant. It is given in the isotropic case by

$$D_\phi = D_2 (1 + l_\phi q^2) + \gamma \frac{1 - \phi_0}{\phi_0} \left(\frac{4}{3} G + B \right) - \gamma \phi_0 \bar{\zeta} = D_1 + D_2 (l_\phi q)^2. \quad (10)$$

Here $D_2 = \gamma \phi_0 (1 - \phi_0) \chi^{-1}$ is the diffusion constant in the absence of elasticity and activity, given in terms of the inverse osmotic susceptibility $\chi^{-1} = \partial \bar{\mu} / \partial \phi$. $l_\phi = \sqrt{2\kappa\chi}$ is the correlation length due to the interfacial tension, i.e., the width of interfaces in the simple binary-mixture case. The $D_2 l_\phi^2 q^2$ term ensures stability for large wave vectors.

The second term accounts for elasticity that drives diffusion in order to relax stresses and network strain [36]. The last term in Eq. (11) results from the active solvent stress and can make the diffusion coefficient negative. This is the case for a contractile stress, $\bar{\zeta} > 0$. The network is then further contracted in cell-rich regions, where it should extend. The $\bar{\zeta}$ term is equivalent to an active relative force proportional

to $\partial_\alpha \phi$ (see Appendix B), which shifts the osmotic susceptibility and can result in a negative diffusion constant. This is the mechanism described by Murray, Oster, and Harris [13, 14]. Our theory in the isotropic case differs from their work mainly because of the global incompressibility that relates the osmotic diffusion constant to elasticity.

Note that the cooperative osmotic diffusion constant is different from the cell self-diffusion constant. The latter describes correlations in the single-cell velocity, while the former describes correlations in the relative current that depends also on concentration. Alternatively, these diffusion constants are different because the random motion of cells does not necessarily result in concentration changes.

The question is whether the osmotic diffusion constant can become negative for reasonable values of the physical parameters of the cells in the ECM. We examine the different contributions to D_1 for $q = 0$. They are all proportional to the mobility, multiplied by different energy-density scales: χ^{-1} , G and B , and the active stress $\bar{\zeta}$. We estimate (see Appendix D) χ^{-1} and the active stresses to be of order 0.1 kPa. The elastic moduli of the ECM, on the other hand, can range between 0.1 and 10 kPa [37, 38]. This means that $D_1 < 0$ is possible only for flexible networks with moduli of the order of 0.1 kPa. Note that in the polar case, even for $D_1 < 0$, other mechanisms can stabilize the system (see Sec. 7).

6. Rigid case: matrix stiffness always stabilizes the ECM, while strain-polarization alignment may destabilize it.

The osmotic diffusion coefficient depends on the elastic moduli. For large moduli, it scales as $\sim \gamma G$ and suppresses concentration gradients. This infers stability in the isotropic case, but not necessarily in the polar case. We verify whether alignment mechanisms can destabilize the system in this limit or not.

In the rigid limit, one solution to the dispersion relation is simply $s = -D_\phi/l_\eta^2$ (see Appendix C). This corresponds to stable concentration fluctuations with a decay rate that is comparable with the largest of τ and $\bar{\tau}$. The other solutions solve

$$0 = (\tau s)^2 + \left[1 + \tau \left(\lambda j_0 + D_p q^2 - \frac{1}{2} \phi_0^2 (1 - \phi_0)^2 \frac{\psi}{G} \bar{\psi} \right) \right] \tau s + \tau (\lambda j_0 + D_p q^2 + \bar{\psi} u_p(0)) \quad (11)$$

The system is unstable if either the constant term or the linear coefficient of the quadratic equation is negative.

We examine the signs of the different contributions in Eq. (11). The λj_0 term is expected to be positive. The steady-state current $j_0 < 0$ for cells that move in the direction of their polarization, and $\lambda < 0$ for cells that align with their direction of motion. The angular diffusion term $D_p q^2$ is also positive. As we consider passive alignment with $\bar{\psi} = -2\psi/\gamma_1$, the last term is positive as well. All together, this yields a positive linear coefficient.

The remaining term is $\bar{\psi} u_p(0)$ in the constant term, where $u_p(0)$ describes network displacement in the x -direction due to polarization changes. It is purely active and given

by

$$u_p(0) = \frac{1}{2}\phi_0(1-\phi_0)\frac{(1-\phi_0)\zeta + \gamma_1\lambda j_0}{G}. \quad (12)$$

These terms are active components of the shear stress. The first stems from the active solvent nematic stress and the latter from the convective polarization stress (shear alignment) in the presence of permeation-alignment and an active current. In the rigid limit of large G , $u_p(0)$ is negligible. This means that the constant term is positive as well, and the system is stable.

The strain-polarization coupling can still have an effect in the rigid limit, as long as ψ/G is of finite magnitude. This is possible. For nematic elastomers, for example, ψ/G can be related to a typical angle between segments, while G is related to the number of crosslinks [26]. As this ratio is at most of order unity within linear elasticity, we use hereafter the value $\phi_0(1-\phi)\psi \approx -0.1G$. According to Eq. (12), $u_p(0) > 0$, unless the cells are sufficiently extensile ($\zeta < 0$). While active cellular stresses are partially contractile ($\zeta > 0$) due to the stresses in the cytoskeleton, they can still be overall extensile, as a result of anisotropic cell division [34] and intercellular interactions [39]. For reasonable values of the active stress and migration velocity (see Appendix D), $u_p(0)$ can become negative only for sufficiently small values of the permeation-alignment coupling $|\lambda| < 2 \times 10^{-2}/\mu\text{m}$. Furthermore, in order for the constant term in Eq. (11) to become negative, the permeation alignment should be even smaller $|\lambda| < 2 \times 10^{-3}/\mu\text{m}$. In this case, the instability occurs for small wave vectors up until it is stabilized by angular diffusion.

The ECM, therefore, is expected to be stable in the rigid limit, unless three conditions are fulfilled: a) cells are sufficiently extensile; b) the strain-polarization coupling is of the same order of magnitude as the matrix stiffness; c) the permeation-alignment parameter is small in absolute value. Note that the third alignment mechanism, concentration alignment, is negligible in this limit, because concentration gradients are suppressed by the large osmotic diffusion coefficient.

We estimate the relaxation time in the stable case. The retardation time for collagen gels that mimic the ECM are of order of minutes [12]. The polarization rates that appear in Eq. (11) are of order of h^{-1} (see Appendix D). This allows to expand Eq. (11) to find $s \approx -1/\tau$ and $s \approx -(\lambda j_0 + D_p q^2 + \bar{\psi} u_p(0))$. Together with the pure concentration mode, this means that two modes decay on the scale of minutes, and a third mode that is related to the polarization on the scale of hours.

7. Analysis in the general case

We analyze the stability in the general case and focus on the stability-instability crossover with zero frequency, $s = 0$. The retardation times, which enter the theory via terms linear in s , do not play any role in this analysis. The determinant of the linear system in Eqs. (8) and (9) is then given by a quadratic equation, $s^2 + 2B(q)s + C(q) = 0$.

The $s = 0$ crossover is defined by setting $C = 0$. Explicitly, this condition is given by

$$\frac{l_\phi^4 k_\phi}{D_2 D_p} (\bar{\psi} - \lambda j_u) u_p(0) + ax + bx^2 + x^3 = 0, \quad (13)$$

where $x = l_\phi^2 q^2$. The system is unstable when the left-hand side is negative. The coefficients are given by

$$a = \frac{l_\phi^2 k_\phi}{D_2} \left[1 + \lambda (\lambda - l_p^{-1}) l_{\gamma_1}^2 + \frac{D_1 \bar{\psi} u_p(0) + \lambda j_0}{D_p k_\phi} - \frac{(1 + \lambda^2 l_{\gamma_1}^2) j_0 + (j_u + \lambda l_{\gamma_1}^2 \bar{\psi}) u_p(0)}{l_p k_\phi} \right],$$

$$b = \frac{l_\phi^2}{D_p} (\bar{\psi} u_p(0) + \lambda j_0) + \frac{D_1 - l_{\gamma_1}^2 l_p^{-2} D_p}{D_2}. \quad (14)$$

Here we have defined $D_\phi = D_1 + D_2 l_\phi^2 q^2 - \lambda l_p^{-1} l_{\gamma_1}^2 D_p$. D_1 is given by the q^0 terms in Eq. (10), with slight modifications due to the strain-polarization coupling (see Appendix B). Note that the x^3 interfacial-tension term stabilizes the system for large wave vectors.

7.1. Strain-polarization coupling stabilizes (destabilizes) contractile (extensile) cells in the ECM for small wave vectors.

The stability for small wave vectors is determined by the sign of the constant term in Eq. (13) $\sim k_\phi (\bar{\psi} - \lambda j_u) u_p(0)$. This term is active. It occurs because both the concentration and polarization are not pure hydrodynamic modes and have a finite relaxation rate for $q = 0$. The concentration, which is a conserved quantity in passive systems, has a finite relaxation rate due to cell division. The polarization, which is usually a soft mode, is coupled to the strain and has a finite relaxation/growth rate due to active shear stresses that polarization rotation imposes on the network.

The question is whether this constant term stabilizes the ECM or destabilizes it. As was shown above, cells that align with matrix segments yield $\bar{\psi} > 0$. Contractile cells have $u_p(0) > 0$, while sufficiently extensile cells have $u_p(0) < 0$. The remaining term to examine is the strain-induced relative current, $j_u = \gamma (2\lambda\phi_0 (1 - \phi_0) \psi - \nu')$. The first term is positive for parallel cell-network alignment ($\psi < 0$) and cells that align with their direction of motion ($\lambda < 0$). The ν' term is expected to be negative, similarly to ν , such that the cells flow in their direction of polarization. This can also be attributed to a strain-dependent friction coefficient (see Appendix B). This yields $j_u > 0$.

Overall, the constant term has the same sign as $u_p(0)$. This means that the net effect of cell division and several alignment mechanisms depends mostly on the sign of the active stress. For contractile cells and weakly extensile cells, the combined effects facilitate a homogeneous, steady flow. For sufficiently extensile cells, an instability can occur, during which large domains of different concentrations and polarizations form. A similar version of this instability was described in Ref. [24] for active, uniaxial, elastomeric gels. The mechanism behind this instability is nematic in nature. It can be understood heuristically by considering a fluctuation in the orientation of active nematic cells (Fig. 2). As the cells rotate, the mesh deforms elastically in order to

balance the cellular active stress. Extensile cells deform the mesh in a way that aligns it parallel with the cells. This drives the rotation of additional cells, because of the aligning interaction. Such a positive feedback infers an instability. Contractile cells, on the other hand, deform the mesh in a way that aligns it perpendicularly to the cells. This drives alignment in the normal direction and relaxes the fluctuation.

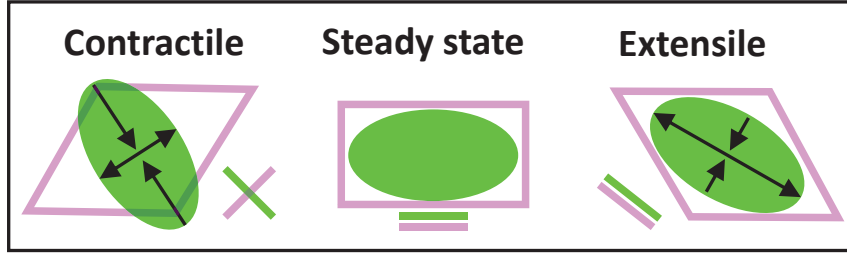


Figure 2: (Color online) Heuristic description of matrix mesh (purple) deformation by the rotation of active, nematic cells (green). The black arrows indicate the direction of forces exerted by the cells. At steady state (center), the cells and matrix are aligned. As contractile cells rotate (left), the matrix deforms and aligns normal to the cells. As extensile cells rotate (right), the matrix deforms and aligns parallel to the cells. Cell and matrix orientations are indicated by the small green and purple lines.

The scaling of the domain size in the unstable case depends on other system parameters. In the simple case where $a > 0$, the most unstable mode is $q = 0$ and system-size domains form for sufficiently large systems. For a negligible permeation-alignment coupling ($\lambda = 0$), the critical system size is $L_c = l_a / \sqrt{-\phi_0(1 - \phi_0)\psi/G}$, where $l_a = 2\pi\sqrt{K/|\zeta|}$ is the active length. A similar scaling appears in the more general analysis below (see Sec. 7.4), as well as other active flow instabilities in nematic cells [40]. Reasonable values of the physical parameters (see Appendix D) yield L_c of the order of $100 \mu\text{m}$. The growth rate is found from the $q = 0$ limit of Eq. (9). It can be approximated as $\phi_0(1 - \phi_0)\psi\zeta / (G\gamma_1)$. Our estimates (see Appendix D) yield a growth time of approximately 100 h. It is shorter for extensile active stresses that are larger than 0.1 kPa or more negative values of $\phi(1 - \phi)\psi/G < -0.1$. The latter limit infers strains of order 1 and a quantitative treatment of it would require a framework of nonlinear elasticity.

Extensile cells can induce an instability also via the term $\sim \bar{\psi}u_p(0)D_1/D_p$ in a . This requires large D_1/D_p values and was described as part of the rigid-limit analysis in Sec. 6. Below, we focus on the contractile case.

7.2. Concentration alignment can stabilize or destabilize the ECM.

We now analyze Eq. (13) for arbitrary q values. The system is unstable when LHS is negative. As $x > 0$, this requires either $a < 0$ or $b < 0$. Reviewing Eq. (14), we find that the only possible source of instability, aside from $D_1 < 0$, is concentration alignment.

Concentration alignment can destabilize the system via three mechanisms. The first mechanism is the term $\lambda(\lambda - l_p^{-1})$ in a that originates from the effective angular diffusion coefficient, $[1 + \lambda(\lambda - l_p^{-1})l_{\gamma 1}^2]D_p$. For sufficiently negative l_p^{-1} , the angular diffusion coefficient becomes negative. While this is a passive mechanism, it has an effect only in the active case where $k_\phi > 0$.

The second mechanism is the term $\sim l_p^{-1}(\lambda - l_p^{-1})$ in b . This is a known passive instability mechanism, where the concentration-alignment coupling favors gradients in concentration and polarization [41, 42, 30] over a homogeneous state. It depends on l_p^{-2} and not on the sign of l_p .

The third mechanism is described by the last terms in a in Eq. (14). The j_0 term is responsible for the active instability reported in Ref. [25]. Consider a concentration fluctuation. The sign of l_p determines whether cells orient into or out of cell-rich regions ($l_p < 0$ or $l_p > 0$, respectively, and see Fig. 1). Cells with $l_p < 0$ actively flow in the direction of their polarization, resulting in an instability.

The $l_p > 0$ case may also become unstable due to the strain-induced current, $j_u > 0$. For sufficiently large j_u , cells would move in the yz plane oppositely to how they re-orient. However, for reasonable physical values (see Appendix D), the j_u term is negligible compared with the j_0 term. Overall, $l_p < 0$ is expected to be destabilizing, while $l_p > 0$ is expected to be stabilizing, except for when $D_p l_{\gamma 1}^2 l_p^{-2} > D_1$.

7.3. Stability diagrams

So far we have identified destabilizing terms. We now precise the instability condition. Eq. (13) is a cubic equation with positive free and cubic coefficients. For it to become negative, it must have a minimum point for some $x_0 = (q_0 l_\phi)^2 > 0$ that has a negative value, as is illustrated in Fig. 4(a). Equating $C'(q_0) = 0$ yields $x_0 = -b/3 \pm \sqrt{(b/3)^2 - a/3}$. We further require its value to be negative, i.e., $C(q_0) < 0$.

These conditions enable to determine the stability of the system. We focus on flexible matrices, such that an instability is possible, and substitute reasonable physical values for cells in the ECM. An important variable to take into account is the mobility γ that appears in most of the terms in Eqs. (13) and (14). It is related to the matrix architecture and is expected to scale as $\gamma \sim \xi^2$. Namely, the active alignment mechanism $\sim j_0/l_p$ in the a term of Eq. (14) is more important for smaller ξ values. As ξ becomes larger, its contributions becomes negligible with respect to osmotic diffusion and permeation alignment.

Our results are presented in Fig. 3 using stability diagrams in the $(\lambda l_\phi, l_\phi/l_p)$ parameter space. We define $D_1 = \gamma \tilde{G} K / l_\phi^2$ and draw three different diagrams for three values of the dimensionless \tilde{G} . Each diagram illustrates stable (white) and unstable (colored) regions for two different mesh sizes, $\xi/l_\phi = 1, 5$.

Figures 3(a) and (b) show that the system is generally unstable for a negative osmotic diffusion constant. The system may still be stable for sufficiently large l_p^{-1} and negative λ values. This is thanks to the stabilizing couplings to the active relative

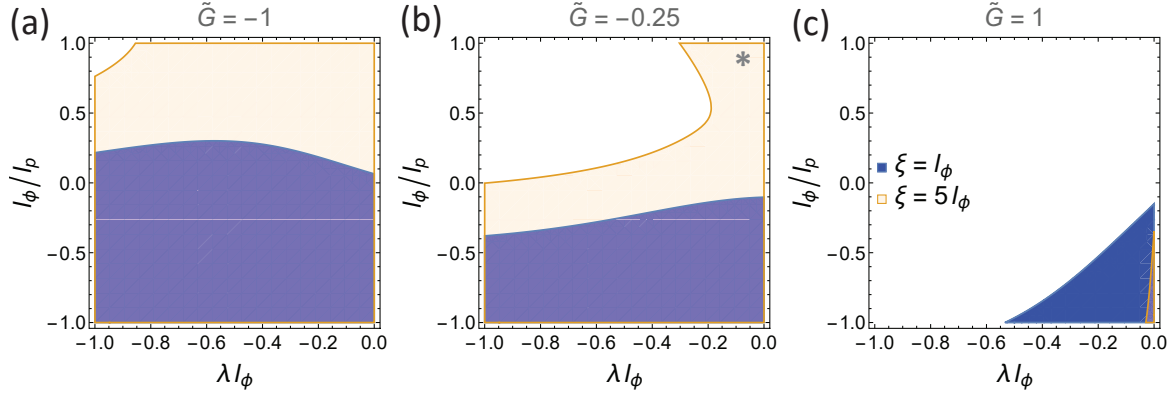


Figure 3: (Color online). Stability diagrams for $\xi = l_\phi$ (blue) and $\xi = 5l_\phi$ (light orange) and different osmotic diffusion constants $\sim \gamma \tilde{G}$. Colored regions are unstable. The values $D_p = 2.5 l_\phi^2 k_\phi$, $\bar{\psi} = 0.25 k_\phi$, $j_0 = -10 l_\phi k_\phi$, and $j_u = (10 l_\phi - 0.25 \lambda \xi^2) k_\phi$ are used, in accordance with the estimates of Appendix D. The asterisk sign in Fig. (b) marks the region where the passive concentration-alignment instability takes place. The other regions correspond to active instabilities.

current and the large effective angular diffusion coefficient. The system is harder to stabilize for more negative \tilde{G} values and larger ξ values, which yield a more negative osmotic diffusion constant. The region in the top right corner of Fig. 3 (b), which is marked with an asterisk sign, is unstable due to the passive concentration-alignment mechanism that occurs for $D_p l_\phi^2 l_p^{-2} > D_1$. This region remains unstable for $\tilde{G} < 0.5$. Figure 3(c) demonstrates that the system is relatively stable for $\tilde{G} > 0$. The system is more susceptible for instabilities for $\xi = l_\phi$, where the stabilizing osmotic diffusion coefficient is smaller. The instability is the active concentration-alignment instability of Sec. 7.2. Note that it occurs for small λ values in absolute values. For more negative λ values, the permeation-alignment mechanism stabilizes the system.

7.4. Critical wave vector

As the system is stable for both vanishing and large wave vectors, all the aforementioned instabilities occur at finite wave vectors. At the critical system parameters, there is only one marginally stable, critical wave vector q_c . This is illustrated in Fig. 4(a). The critical wave vector is found from $C(q_c) = C'(q_c) = 0$, where $C(q)$ is the polynomial in Eq. (13).

We find q_c in the reasonable limit where the constant term of Eq. (13) is small, i.e., $0 < \frac{l_\phi^4}{D_2 D_p} k_\phi (\bar{\psi} - \lambda j_u) u_p(0) \ll 1$. The solution depends on the sign of a that is defined in Eq. (14). It is given by

$$\begin{aligned}
 q_c l_\phi &= a^{1/4} & a > 0, \\
 q_c l_\phi &= \left(-2 \frac{l_\phi^4 k_\phi}{D_2 D_p} (\bar{\psi} - \lambda j_u) \frac{u_p(0)}{a} \right)^{1/2} & a < 0.
 \end{aligned} \tag{15}$$

In the isotropic limit, $a = l_\phi^2 k_\phi / D_2$, and our result reduces to that of Oster et al. [13, 14]. This is a generic scaling for phase separation of reproducing entities (see also Ref. [43] for pattern formation in bacteria). In the polar case, while the scaling $q \sim (k_\phi / D_2)^{1/4}$

still holds, the prefactor can change substantially due to alignment mechanisms. This is illustrated in Fig. 4(b) as a function of l_p for $\lambda = 0$. a decreases as l_p becomes more negative and, consequently, the critical wave vector decreases as well. It becomes infinitesimally small as a approaches zero.

The second line in Eq. (15) arises due to the active concentration-alignment mechanism. We focus on the $\lambda = 0$ case and plot the critical wave vector for different l_p values in Fig. 4(c). It is possible to estimate it in the limit where $-j_0/(l_p k_\phi)$ is the dominant contribution to a . This yields the scaling

$$q_c \sim \sqrt{-\frac{\psi l_p k_\phi \zeta}{G j_0 K}}. \quad (16)$$

Namely, the critical wavelength is proportional to the active length l_a . The critical wave vector is expected to be small in this limit, as is evident from Fig. 4(c).

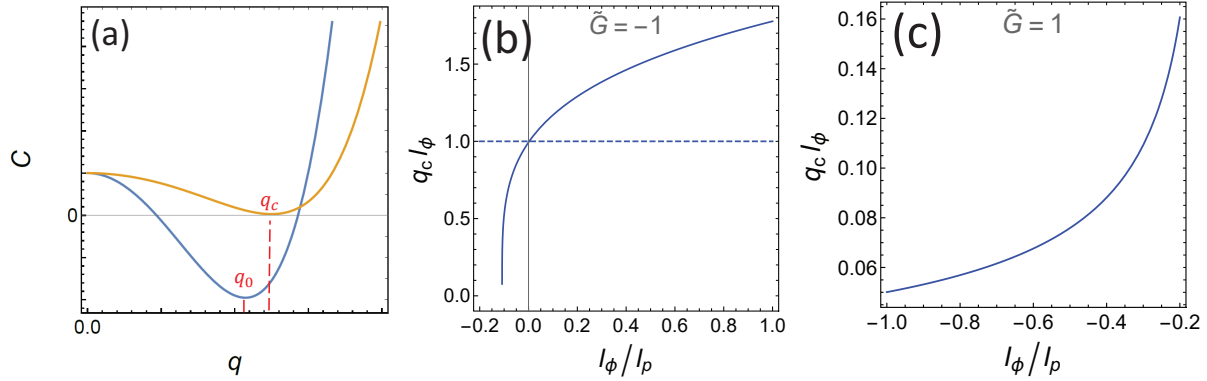


Figure 4: (Color online). (a) $C(q)$ in arbitrary units. The system is unstable for $C < 0$. The wave vector q_0 is found as a negative, minimal point, while the critical wave vector q_c is a degenerate root. (b) Critical wave vector as a function of l_p^{-1} in the case $a > 0$ for $\tilde{G} = -1$. The result in the isotropic case ($l_p^{-1} = 0$) is marked by a dashed line. (c) Critical wave vector as a function of l_p^{-1} in the case $a < 0$ for $\tilde{G} = 1$. The same values as those of Fig. 3 are used with $\xi = l_\phi$.

In addition to the critical wave vector, there is also a fastest growing mode with wave vector q_* , for which s is maximal. This infers the formation of transient periodic domains of size $\sim 1/q_*$ with continuous flow patterns between the domains. This may correspond to the formation of clusters or strands of cells that migrate in localized collections. In standard binary systems, these domains grow into macroscopically phase-separated regions. However, any coarsening dynamics is arrested by cell division and death [43], which does not allow stable macroscopic domains with a concentration that is different from the homeostatic one $\phi \neq \phi_0$.

8. Discussion

In this paper, we have formulated an active-gel theory to describe multicellular migration in the ECM as an active, polar solvent permeating in a viscoelastic solid. The

theory accounts naturally for dynamic reciprocity and classifies clearly different cell-matrix interactions. Namely, we highlight three alignment mechanisms that relate the polarization with the strain ($\sim \psi$), permeation current ($\sim \lambda$) and concentration gradients ($\sim l_p^{-1}$). The three are distinguishable; The ψ coupling, unlike the other two, occurs also for nematic cells and in the absence of concentration gradients and current. It is possible to separate between the permeation- and concentration-alignment mechanisms by studying cells with different motilities and in different setups (e.g., in the bulk of a cell collection, compared to an invading cell front).

A main conclusion of our work regards the effect of cell-matrix alignment on the stability of homogeneous multicellular migration for small wave vectors. Confluent cell monolayers can be extensile or contractile depending on the cell type and the regulation of cell-cell adhesions [39]. Our results indicate that cells with different values of the active stress would migrate in qualitatively different manners within a three-dimensional matrix. Contractile and weakly extensile cells flow homogeneously, while sufficiently extensile cells form domains. This simple distinction is remarkable, given the large number of forces and alignment mechanisms that take place. We note that cell-cell interactions in polarized cells that migrate in a fluid-like manner are generally weaker than those in confluent monolayers.

In addition to this strain-driven instability in the extensile case, our analysis suggests two possible origins for instability in the contractile case: a negative, effective diffusion constant, due to active forces, or a negative $l_p < 0$ that aligns cells towards larger cellular concentrations. The value of l_p tunes the critical wave vector of the instability.

While this work focuses on the linear stability of homogeneous polarized cells, our framework could be equally useful in other relevant situations. It could describe, for example, the flow of cell fronts during invasion or an isotropic-polar transition of cells in the ECM. The combination of alignment mechanisms is expected to polarize cells. Namely, cells would flow mainly parallel to network segments, due to anisotropy of friction coefficient, while the polarization and migration speed are expected to feedback via the permeation-alignment mechanism, resulting in polarized, flowing cells.

Another interesting example is cells migrating in tracks of aligned collagen fibers [5, 9]. Concentration gradients are expected to be small in this case, and the flow in the normal direction to the polarization is expected to be negligible. Most of the effects discussed in this work should not be relevant then. This is evident by taking the limit of vanishing mobility. Rather, the cells could be described in this case as a fluid flowing in a confined geometry, similarly to the theoretical description of in-vitro migration experiments in channels (see, e.g., [40]). As cell-matrix friction becomes a boundary effect, the cellular viscous stresses become important in this setup.

Several extensions of our theory can be considered. It is possible to add components to the current two-component description that coarse-grains the solvent and cells together. This overlooks solvent-cell friction, which is reasonable, because the cells are almost ten orders of magnitude more viscous than water and thus dominate the

dissipative processes. The description becomes problematic, however, when the cellular concentration is inhomogeneous across the solvent. For example, when contractile cells are added to a pre-existing gel, they contract it and squeeze out some of the solvent. This can be described in our two-component theory only in an indirect way, by varying the value of the active stresses. Second, this framework overlooks diverse cell species, such as cancer cells vs. fibroblasts. Fibroblasts are especially interesting because they are abundant in the ECM and are able to remodel it. Active matrix remodeling is currently missing from our theory. The theory can also be adapted for more complicated rheological descriptions of the ECM [11], including plasticity, long-time stress relaxation and non-linearities. A treatment of the latter two within the same framework can be found in [25], where we considered also reversible network deformation by the migration current (“permeation deformation”). We reserve the further study of this effect and active remodeling to a future work.

In conclusion, this work could open an avenue for studying cell-migration modes, ECM patterning, and cell-ECM interactions in three dimensions and at the mesoscopic scale. Thanks to the generic framework, it can be used to study other physical systems, such as bacteria and active colloids in viscoelastic media. It would be interesting to apply our theory to three-dimensional migration experiments that measure cell concentration, alignment and velocity in the ECM or engineered gels. We suggest to compare between the migration of extensile and contractile cells and to verify whether domains form for sufficiently extensile cells. In addition, measuring and deducing typical values of l_p for different cell types should be important in characterizing their migration modes.

Acknowledgments

RMA acknowledges funding from Fondation pour la Recherche Médicale (FRM Postdoctoral Fellowship).

Appendix A. Polarization-rate constitutive equation

We make use of the general framework of non-equilibrium thermodynamics, similarly to Ref. [25]. We start from the general equation for the polarization dynamics

$$(\partial_t + v_\beta^c \partial_\beta) p_\alpha - p_\beta \partial_\beta v_\alpha^c = \frac{1}{\gamma_1} h_\alpha + \lambda j_\alpha + \phi (1 - \phi) \psi' \Delta \mu \epsilon_{\alpha\beta} p_\beta. \quad (\text{A.1})$$

The derivative on the left-hand side is a material derivative and a convective term. The cells are assumed to convect by their own velocity and rotate due to their strain-rate like rigid rods (shear-alignment parameter of -1). The right-hand side accounts for dissipative couplings. The coupling to the orientational field $h_\alpha = -\delta F / \delta p_\alpha$ is given in terms of the rotational viscosity γ_1 . The coupling to the relative current, j_α is referred to as the permeation-alignment coupling. The coupling to activity $\Delta \mu$ includes the strain (a term $\sim \Delta \mu p_\alpha$ simply renormalizes the parallel field, h_{\parallel}) and is proportional to $\phi (1 - \phi)$, because it involves interaction with the matrix.

The orientational field is given by

$$h_\alpha = h_\parallel p_\alpha + K (\partial_\beta \partial_\beta p_\alpha + l_p^{-1} \partial_\alpha \phi) - 2\phi (1 - \phi) \psi \epsilon_{\alpha\beta} p_\beta. \quad (\text{A.2})$$

Substituting in Eq. (A.1) yields Eq. (3) with $\bar{h}_\parallel = h_\parallel/\gamma_1$, $D_p = K/\gamma_1$, and $\bar{\psi} = \psi' \Delta\mu - 2\psi/\gamma_1$. We consider hereafter $\psi' = 0$, such that strain-polarization alignment is driven by the passive free-energy coupling, $\bar{\psi} = -2\psi/\gamma_1$.

Appendix B. Linearization of the dynamic equations

In this Appendix we derive the linearized version of the equations, which is used for the linear stability analysis. We first write the equations in full form, including explicit expressions for the fields that are derived from the free energy. Then, we solve the steady-state equations, and linearize around the steady-state solution.

Matrix forces

The dynamic equations include force-balance equations, written in terms of the cell and matrix forces. The matrix force is given in Eq. (5). It includes the divergence of the elastic stress,

$$\sigma_{\alpha\beta}^{el} = \frac{\delta F}{\delta \epsilon_{\alpha\beta}} = \frac{\phi}{\phi_0} (2G\tilde{\epsilon}_{\alpha\beta} + B\epsilon\delta_{\alpha\beta}) + \phi (1 - \phi) \psi Q_{\alpha\beta}. \quad (\text{B.1})$$

In addition, it includes the force that results from osmotic pressure gradients, $-\phi\partial_\alpha\bar{\mu}$. The relative chemical potential is given by

$$\begin{aligned} \bar{\mu} &= \frac{\delta F}{\delta \phi} = -k_B T a^{-3} (1 + \ln(1 - \phi)) + (1 - 2\phi) (\chi_0 + \psi Q_{\alpha\beta} \epsilon_{\alpha\beta}) \\ &\quad + G\tilde{\epsilon}^2 + \frac{1}{2} B\epsilon^2 + K l_p^{-1} \partial_\alpha p_\alpha - 2\kappa \partial_\beta \partial_\beta \phi. \end{aligned} \quad (\text{B.2})$$

Steady state

We consider a homogeneous steady-state, as is described in Sec. 4. For a homogeneous system, the forces acting on the cells and matrix [Eqs. (5) and (6)] vanish. Force balance then requires that the relative force vanishes as well, i.e.,

$$\frac{1}{\gamma} j_\alpha^0 = \phi_0 (1 - \phi_0) \left(\lambda h_\alpha^0 + \left[\nu - \nu' \frac{\psi}{3G} \phi_0 (1 - \phi_0) \right] p_\alpha^0 \right). \quad (\text{B.3})$$

The steady-state molecular field results from the active relative and is given by

$$h_\alpha^0 = -\gamma_1 \lambda j_\alpha^0. \quad (\text{B.4})$$

Inserting this result in the previous equation yields the relative current at steady state,

$$j_\alpha^0 = \frac{\gamma}{1 + \lambda^2 l_{\gamma_1}^2} \phi_0 (1 - \phi_0) \left[\nu - \nu' \frac{\psi}{3G} \phi_0 (1 - \phi_0) \right] p_\alpha^0, \quad (\text{B.5})$$

where $l_{\gamma_1} = \sqrt{\phi_0 (1 - \phi_0) \gamma_1 \gamma}$ is a screening length due to the interplay between friction and rotational viscosity. We consider $\nu, \nu' < 0$, such that the cells migrate in the direction of their polarization. The role of ν' at steady state is to renormalize the motility. The permeation-alignment mechanism effectively increases the friction.

Linearized equations

The stability is studied by introducing a small perturbation in the fields at point r_α and time t with a wave vector q_α and growth rate s ,

$$(\phi, p_\alpha, u_\alpha) \approx (\phi_0, p_\alpha^0, u_\alpha^0) + (\phi^1, p_\alpha^1, u_\alpha^1) \exp(iq_\alpha r_\alpha + st). \quad (\text{B.6})$$

For simplicity, we consider $q_x = 0$. Also, in order to maintain the modulus of the polarization, $p_x^1 = 0$. As is explained in the paper, it is possible to integrate over the displacement variable and to analyze the stability in terms of ϕ^1 and $p_d^1 = iq_\alpha p_\alpha^1$.

The linearized continuity equation [Eq. (2)] is given by

$$s\phi^1 = -iq_\alpha j_\alpha^1 - k_\phi \phi^1. \quad (\text{B.7})$$

The linearized equation for the polarization [divergence of Eq. (3)] reads

$$\begin{aligned} sp_d^1 = & \bar{h}_\parallel p_d^1 - D_p q^2 p_d^1 - D_p l_p^{-1} q^2 \phi^1 + \lambda iq_\alpha j_\alpha^1 \\ & + \phi_0 (1 - \phi_0) \bar{\psi} iq_\alpha (\epsilon_{\alpha\beta} p_\beta)^1. \end{aligned} \quad (\text{B.8})$$

The parallel field can be found from the polarization-rate equation at steady state, $\bar{h}_\parallel = -\lambda j_0 + \frac{1}{3}\phi_0^2 (1 - \phi_0)^2 \bar{\psi}\psi/G$. The $iq_\alpha (\epsilon_{\alpha\beta} p_\beta)^1$ term in Eq. (B.8) is given by

$$iq_\alpha (\epsilon_{\alpha\beta} p_\beta)^1 = -\frac{1}{2}q^2 u_x^1 + \frac{\psi}{6G}\phi_0 (1 - \phi_0) p_d^1. \quad (\text{B.9})$$

The displacement in the x -direction is found from the force balance on the entire gel [sum of the two lines in Eq. (4)] in the x -direction. As $q_x = 0$, only the total shear stress of the system contributes to this force. We find that

$$u_x^1 = \frac{1}{G(1 + \tau s)q^2} [(1 - \phi_0)\zeta + \phi_0(1 - \phi_0)\psi - h_x^0] p_d^1. \quad (\text{B.10})$$

This demonstrates how the network is strained by active stresses (ζ term) and alignment mechanisms (h_x^0 term), as well as the stress due to passive alignment (ψ term).

We find that

$$iq_\alpha (\epsilon_{\alpha\beta} p_\beta)^1 = -\frac{1}{\phi_0(1 - \phi_0)} \left(u_p + \frac{1}{3}\phi_0^2 (1 - \phi_0)^2 \frac{\psi}{G} \right) p_d^1, \quad (\text{B.11})$$

where u_p is given by

$$\begin{aligned} u_p &= u_p(0) - \frac{\tau s}{1 + \tau s} \left(u_p(0) + \frac{1}{2}\phi_0^2 (1 - \phi_0)^2 \frac{\psi}{G} \right), \\ u_p(0) &= \frac{\phi_0(1 - \phi_0)}{2G} [(1 - \phi_0)\zeta - h_x^0]. \end{aligned} \quad (\text{B.12})$$

This yields overall

$$sp_d^1 = -(\lambda j_0 + \bar{\psi}u_p + D_p q^2) p_d^1 - D_p l_p^{-1} q^2 \phi^1 + \lambda iq_\alpha j_\alpha^1. \quad (\text{B.13})$$

It remains to find the divergence of the relative current. We take a linear combination of the two force balance equations in Eq. (4) of the paper, and find that

$$\frac{1}{\gamma} iq_\alpha j_\alpha^1 = iq_\alpha (\phi_0(1 - \phi_0) [\lambda h_\alpha^1 + \nu p_\alpha^1 + \nu' (\epsilon_{\alpha\beta} p_\beta)^1] + (1 - \phi_0) f_\alpha^{m1} - \phi_0 f_\alpha^{c1}). \quad (\text{B.14})$$

Before resuming the calculation, we note that the active relative force $\sim \nu'$ plays, in part, a similar role to an anisotropic friction coefficient. To see this, consider a friction coefficient $\gamma_{\alpha\beta}^{-1} = \gamma_0^{-1}\delta_{\alpha\beta} + \gamma_\epsilon^{-1}\epsilon_{\alpha\beta}$. Then, expanding the friction force would yield

$$(\gamma_{\alpha\beta}^{-1}j_\beta)^1 = \left[\gamma_0^{-1}\delta_{\alpha\beta} - \frac{\psi}{2G}\phi_0(1-\phi_0)Q_{\alpha\beta}^0\gamma_\epsilon^{-1} \right] j_\beta^1 + \gamma_\epsilon^{-1}j_0\epsilon_{\alpha x}^1. \quad (\text{B.15})$$

It is evident that the correction $\sim \epsilon_{\alpha x}^1$ appears in a similar way either due to γ_ϵ^{-1} or ν^1 . Explicitly this yields the relation $\nu' = -\gamma_\epsilon^{-1}j_0$. For $j_0 < 0$ and considering that the friction is expected to decrease due to network alignment, we conclude that ν' is indeed expected to be negative, as was mentioned above.

We return to the calculation of the divergence of the relative current and examine each contribution separately. For the orientational field, we find that

$$iq_\alpha h_\alpha^1 = -K(q^2 p_d^1 + l_p^{-1}q^2 \phi^1) + h_{\parallel}^0 p_d^1 - 2\phi_0(1-\phi_0)\psi iq_\beta(\epsilon_{\alpha\beta} p_\beta)^1. \quad (\text{B.16})$$

The last contribution appears also in the ν' term. Summing the two contributions leads to $j_u(u_p + \frac{1}{3}\phi_0^2(1-\phi)^2\frac{\psi}{G})p_d^1$, where $j_u/\gamma = -\nu' + 2\lambda\phi_0(1-\phi_0)\psi$ describes the two contributions to the strain-dependent relative forces: the active relative force $\sim \nu'$ and the permeation-alignment mechanism $\sim \lambda$, which includes polarization alignment to the strain. We further simplify using the steady-state equation for the current,

$$\frac{1}{3}\phi_0^2(1-\phi)^2\frac{\psi}{G}j_u + \gamma\phi_0(1-\phi_0)(\lambda h_{\parallel} + \nu) = j_0. \quad (\text{B.17})$$

For the matrix force, we calculate separately the contributions of the elastic stress and osmotic pressure. The elastic contribution is

$$\begin{aligned} -q_\alpha q_\beta \sigma_{\alpha\beta}^{el,1} &= -q_\alpha q_\beta \left[2G\tilde{\epsilon}_{\alpha\beta}^1 + B\epsilon^1\delta_{\alpha\beta} + 2\phi_0(1-\phi_0)\psi p_\alpha^1 p_\beta^0 + (1-2\phi_0)\psi Q_{\alpha\beta}^0 \phi^1 + 2\frac{\phi^1}{\phi_0}G\tilde{\epsilon}_{\alpha\beta}^0 \right] \\ &= \left[\frac{1}{\phi_0} \left(\frac{4}{3}G + B \right) - \frac{1}{3}\phi_0\psi \right] q^2 \phi^1, \end{aligned} \quad (\text{B.18})$$

where we have made use of the fact that $\epsilon^1 = -\phi^1/\phi_0$ and $q_x = 0$. The contribution from the osmotic pressure is

$$\begin{aligned} \phi_0 q^2 \bar{\mu}^1 &= \phi_0 q^2 \left[\frac{k_B T}{a^3} \frac{\phi^1}{1-\phi_0} - 2(\chi_0 + \psi Q_{\alpha\beta}^0 \epsilon_{\alpha\beta}^0) \phi^1 + (1-2\phi_0)\psi(Q_{\alpha\beta}^0 \epsilon_{\alpha\beta}^1 + 2p_\alpha^1 p_\beta^0 \epsilon_{\alpha\beta}^0) \right. \\ &\quad \left. + \frac{2}{\phi_0}G\tilde{\epsilon}_{\alpha\beta}^1 \tilde{\epsilon}_{\alpha\beta}^0 + Kl_p^{-1}p_d^1 + 2\kappa q^2 \phi^1 \right] \\ &= \phi_0 q^2 \left[\frac{k_B T}{a^3} \frac{1}{1-\phi_0} - 2\chi_0 + \frac{2\psi^2}{3G}\phi_0(1-\phi_0) - \frac{1}{3}\psi + 2\kappa q^2 \right] \phi^1 + \phi_0 Kl_p^{-1} q^2 p_d^1. \end{aligned} \quad (\text{B.19})$$

Together this yields

$$iq_\alpha f_\alpha^{m1} = \left[\frac{1}{\phi_0} \left(\frac{4}{3}G(1+\tau s) + B(1+\bar{\tau} s) \right) + \phi_0 \chi^{-1}(1+l_\phi^2 q^2) \right] q^2 \phi^1 + \phi_0 Kl_p^{-1} q^2 p_d^1. \quad (\text{B.20})$$

where we have defined the effective inverse susceptibility

$$\chi^{-1} = \frac{k_B T}{a^3} \frac{1}{1-\phi_0} - 2 \left(\chi_0 + \frac{\psi}{3} \right) + \frac{2\psi^2}{3G}\phi_0(1-\phi_0), \quad (\text{B.21})$$

and the interfacial correlation length $l_\phi = \sqrt{2\kappa\chi}$. Note that parallel cell-strain alignment ($\psi < 0$) has a positive contribution.

For the cellular force, we find that

$$iq_\alpha f_\alpha^{c1} = \left(\bar{\zeta} - \frac{1}{3}\zeta \right) q^2 \phi^1. \quad (\text{B.22})$$

Note that the isotropic $\bar{\zeta}$ stress does not affect the total stress, due to incompressibility. It simply renormalizes the pressure δP . Its only role is in the equation for the relative current [Eq. (B.14)] and it can be interpreted as an active, relative force $\sim \partial_\alpha \phi$.

Inserting back in the equation for the current yields overall

$$iq_\alpha j_\alpha^1 = (D_\phi + l_\eta^2 s) q^2 \phi^1 + [(l_p^{-1} - \lambda) l_{\gamma 1}^2 D_p q^2 + j_0 + j_u u_p] p_d^1. \quad (\text{B.23})$$

Here we have defined the effective osmotic diffusion constant as $D_\phi = D_1 + D_2 l_\phi^2 q^2 - \lambda l_p^{-1} l_{\gamma 1}^2 D_p$ with

$$\begin{aligned} D_1 &= \gamma \phi_0 (1 - \phi_0) \chi^{-1} + \gamma \frac{1 - \phi_0}{\phi_0} \left(\frac{4}{3} G + B \right) + \gamma \phi_0 \left(\frac{1}{3} \zeta - \bar{\zeta} \right), \\ D_2 &= \gamma \phi_0 (1 - \phi_0) \chi^{-1}, \end{aligned} \quad (\text{B.24})$$

as well as $l_\eta = \sqrt{\gamma \frac{1 - \phi_0}{\phi_0} \left(\frac{4}{3} G \tau + B \bar{\tau} \right)}$, a screening length due to the interplay between friction and transient matrix viscosity. This diffusion constant differs from that in the isotropic case [Eq. (10)] in two ways: its inverse susceptibility has contributions $\sim \psi$ [Eq. (B.21)], and it includes the nematic active stress $\sim \zeta$.

Inserting Eq. (B.23) in Eqs. (B.7) and (B.13) yields the linearized dynamic equations, Eqs. (8) and (9).

Appendix C. Linear stability in the rigid limit

In the rigid matrix limit, concentration fluctuations generate a large free-energetic cost, and D_ϕ becomes very large. For a finite retardation time, l_η^2 becomes very large as well. We consider a finite system size L and a minimal wave vector $q_m = 2\pi/L$, such that $l_\eta^2 q_m^2 \gg 1$ and $D_\phi q_m^2 \gg k_\phi$. In this approximation, Eqs. (8) and (9) reduce to

$$\begin{aligned} 0 &= (D_\phi + l_\eta^2 s) q^2 \phi^1 + [(l_p^{-1} - \lambda) l_{\gamma 1}^2 D_p q^2 + j_0 + j_u u_p] p_d^1 \\ 0 &= [s + (\bar{\psi} - \lambda j_u) u_p + (1 + \lambda (\lambda - l_p^{-1}) l_{\gamma 1}^2) D_p q^2] p_d^1 - \lambda (D_\phi + l_\eta^2 s) q^2 \phi^1. \end{aligned} \quad (\text{C.1})$$

One solution is $s = -D_\phi/l_\eta^2$, which corresponds to stable concentration fluctuations. The other two possible solutions are found from the remaining factor in the determinant

$$\begin{aligned} 0 &= s + (\bar{\psi} - \lambda j_u) u_p + (1 + \lambda (\lambda - l_p^{-1}) l_{\gamma 1}^2) D_p q^2 + \lambda [(l_p^{-1} - \lambda) l_{\gamma 1}^2 D_p q^2 + j_0 + j_u u_p] \\ &= s + \bar{\psi} u_p + \lambda j_0 + D_p q^2. \end{aligned} \quad (\text{C.2})$$

Substituting u_p [Eq. (B.12)] leads to Eq. (11).

Appendix D. Estimations of parameters

The basic time scale of the theory is $1/k_\phi$. We estimate it as $1/k_\phi = 24\text{h}$ for a typical division time of one day. The basic length scale of the theory is the correlation length l_ϕ . For simplicity, we choose a small length of order of the cell size a that we set as $l_\phi = a = 10\ \mu\text{m}$. This is the lowest value that we consider for length scales, including λ^{-1} , l_p , and ξ . Next, we estimate the remaining parameters of our theory. The estimations are summarized in Table 2.

Osmotic diffusion constant. The diffusion constant D_1 includes terms of the form γG , $\gamma\zeta$, $\gamma\chi^{-1}$ [Eq. (B.24)]. The mobility can be related to the cellular shear viscosity η as $\gamma \approx \xi^2/\eta$, where ξ is a typical mesh size. The viscosity of epithelial monolayers is of order $\eta \approx 10^3 - 10^4\text{Pa h}$ [44]. As our theory coarse grains the cells and solvent together, we consider the value of $\eta = 1\text{ kPa h}$. This value can be regarded as an upper bound of the viscosity. The ECM and collagen gels in general can have a large range of stiffness values in the range $0.1 < G < 10\text{ kPa}$ [37, 38]. For the active stress, we consider a 2D myosin contractility of $\zeta_{2D} \approx 1\text{ kPa } \mu\text{m}$ [45]. Dividing by a typical cell size of $a = 10\ \mu\text{m}$, the cells are expected to exert a stress of order 0.1 kPa . We use this order of magnitude as well for extensile active stresses. For the inverse susceptibility, we make a scaling argument, taking $1/k_\phi$ as the basic timescale of the system. We write the corresponding term in the diffusion constant as $D_2 = \gamma\phi_0(1 - \phi_0)\chi^{-1} \equiv l^2k_\phi$, where l is a lengthscale. The minimal possible l is $l = a$. For a fixed χ , this is obtained for the minimal mobility $\gamma = a^2/\eta$. This yields $D_2 \approx \xi^2k_\phi$ and, consequently, $\chi^{-1} \approx \eta k_\phi \approx 0.1\text{ kPa}$.

Relative current and strain-polarization coupling. The steady-state relative current is estimated by a typical migration velocity [38] $j_0 = 5\ \mu\text{m}/\text{h}$. We also consider the contribution of the strain-induced current around the steady state, $(j_u + \lambda l_{\gamma_1}^2 \bar{\psi}) u_p(0)$. We have $j_u + \lambda l_{\gamma_1}^2 \bar{\psi} = -\gamma\nu'$. The strain-dependent, active, relative force is estimated as $\nu' = -\gamma_\epsilon^{-1}j_0$, assuming that it has a similar effect as a strain-dependent friction coefficient (Appendix B). For simplicity, we consider $\gamma_\epsilon = -\gamma$. This yields $j_u + \lambda l_{\gamma_1}^2 \bar{\psi} = -j_0$. The polarization-induced strain parameter is given by $u_p(0) = \phi_0(1 - \phi_0)[(1 - \phi_0)\zeta + \gamma_1\lambda j_0]/(2G)$. For a small modulus $G = 0.1\text{ kPa}$, we find that $u_p(0) \approx 0.1(1 - 5\lambda l_\phi)$. The strain $u_p(0)$ often appears next to the strain-polarization rate $\bar{\psi} = -2\psi/\gamma_1$. For the strain-polarization coupling ψ , we consider the value $\phi_0(1 - \phi_0)\psi = -0.1G$. The sign signifies that the cells align parallel to network segments and the order of magnitude is the largest possible within the framework of linear elasticity. The product $\bar{\psi}u_p(0)$ is then given by $0.25(1 - 5\lambda l_\phi)k_\phi$, where we have set the rotational viscosity as the shear viscosity, $\gamma_1 = \eta$.

Angular diffusion constant. The angular diffusion constant is $D_p = K/\gamma_1$. The Frank constant in two dimensions K_{2D} can be estimated from experiments that measure the active lengthscale, $l_a = 2\pi\sqrt{K_{2D}/|\zeta_{2D}|}$, where ζ_{2D} is the two-dimensional active, nematic stress. Experiments on cell monolayers have measured a length of order $l_a \approx 50\ \mu\text{m}$ [40]. Considering again a 2D myosin contractility of order $\text{kPa } \mu\text{m}$, we

find that $K_{2D} \approx 100 \text{ kPa } \mu\text{m}^3$. Dividing by the cell size yields $K_{3D} \approx 10 \text{ kPa } \mu\text{m}^2$ and $D_p \approx 10 \mu\text{m}^2/\text{h}$.

Table D1: Estimations of the parameters used in our theory. Ranges of values result from the range of elastic moduli, $0.1 < G < 10 \text{ kPa}$. The screening length l_η is evaluated for large elastic moduli, as in Sec. 6.

Parameter	Estimate	Parameter	Estimate
l_ϕ	$10 \mu\text{m}$	ξ (mesh size)	$l_\phi < \xi < 10l_\phi$
$D_1 \cdot (l_\phi/\xi)^2$	$-10 < \dots < 10^3 \mu\text{m}^2/\text{h}$	$D_2 \cdot (l_\phi/\xi)^2$	$5 \mu\text{m}^2/\text{h}$
k_ϕ	$1/24\text{h}$	D_p	$10 \mu\text{m}^2/\text{h}$
l_η	$l_\eta \approx \xi$	$l_{\gamma 1}$	$l_{\gamma 1} \approx \xi$
$\bar{\psi}$	$10^{-2} < \dots < 1/\text{h}$	u_p	$\bar{\psi}u_p(0) \approx 10^{-2} (1 - 5\lambda l_\phi)/\text{h}$
j_0	$-5 \mu\text{m}/\text{h}$	j_u	$j_u \approx -j_0 - \lambda \xi^2 \bar{\psi}$
l_p	$ l_p > l_\phi$	λ	$0 > \lambda > -1/l_\phi$

- [1] Vincent Hakim and Pascal Silberzan. Collective cell migration: A physics perspective. *Reports on Progress in Physics*, 80, 4 2017.
- [2] Ricard Alert and Xavier Trepat. Physical models of collective cell migration. *The Annual Review of Condensed Matter Physics is Annu. Rev. Condens. Matter Phys.* 2020, 11:77–101, 2019.
- [3] Peter Friedl and Darren Gilmour. Collective cell migration in morphogenesis, regeneration and cancer. *Nature Reviews Molecular Cell Biology*, 10:445–457, 7 2009.
- [4] Peter Friedl, Joseph Locker, Erik Sahai, and Jeffrey E. Segall. Classifying collective cancer cell invasion. *Nature Cell Biology*, 14:777–783, 8 2012.
- [5] Andrew G. Clark and Danijela Matic Vignjevic. Modes of cancer cell invasion and the role of the microenvironment. *Current Opinion in Cell Biology*, 36:13–22, 10 2015.
- [6] Guillaume Charras and Erik Sahai. Physical influences of the extracellular environment on cell migration. *Nature Reviews Molecular Cell Biology*, 15:813–824, 12 2014.
- [7] Jennifer Alexander and Edna Cukierman. Stromal dynamic reciprocity in cancer: Intricacies of fibroblastic-ecm interactions. *Current Opinion in Cell Biology*, 42:80–93, 10 2016.
- [8] Sjoerd Van Helvert, Cornelis Storm, and Peter Friedl. Mechanoreciprocity in cell migration. *Nature Cell Biology*, 20:8–20, 1 2018.
- [9] Weijing Han, Shaohua Chen, Wei Yuan, Qihui Fan, Jianxiang Tian, Xiaochen Wang, Longqing Chen, Xixiang Zhang, Weili Wei, Ruchuan Liu, Junle Qu, Yang Jiao, Robert H. Austin, and Liyu Liu. Oriented collagen fibers direct tumor cell intravasation. *Proceedings of the National Academy of Sciences of the United States of America*, 113:11208–11213, 10 2016.
- [10] Esther Wershof, Danielle Park, Robert P. Jenkins, David J. Barry, Erik Sahai, and Paul A. Bates. Matrix feedback enables diverse higher-order patterning of the extracellular matrix. *PLoS Computational Biology*, 15, 2019.
- [11] Alberto Elosegui-Artola. The extracellular matrix viscoelasticity as a regulator of cell and tissue dynamics. *Current Opinion in Cell Biology*, 72:10–18, 10 2021.
- [12] Andrew Clark, Ananyo Maitra, Cécile Jacques, Anthony Simon, Carlos Pérez-González, Xavier Trepat, Raphaël Voituriez, and Danijela Matic Vignjevic. Viscoelastic relaxation of collagen networks provides a self-generated directional cue during collective migration. 2020.
- [13] J D Murray, G F Oster, and A K Harris. A mechanical model for mesenchymal morphogenesis. *Journal of Mathematical Biology*, 17:125–129, 1983.
- [14] G F Oster, J D Murray, and A K Harris. Mechanical aspects of mesenchymal morphogenesis. *J. Embryol. exp. Morph.*, 78:3, 1983.
- [15] Luke Olsena, Philip K Mainia, Jonathan A Sherratt, and Ben Marchant. Simple modelling of extracellular matrix alignment in dermal wound healing i. cell flux induced alignment.
- [16] John C Dallon, Jonathan A Sherratt, and Philip K Maini. Mathematical modelling of extracellular matrix dynamics using discrete cells: Fiber orientation and tissue regeneration, 1999.
- [17] Steven McDougall, John Dallon, Jonathan Sherratt, and Philip Maini. Fibroblast migration and collagen deposition during dermal wound healing: Mathematical modelling and clinical implications. *Philosophical Transactions of the Royal Society A: Mathematical, Physical and Engineering Sciences*, 364:1385–1405, 6 2006.
- [18] K. J. Painter. Modelling cell migration strategies in the extracellular matrix. *Journal of Mathematical Biology*, 58:511–543, 4 2009.
- [19] J. F. Joanny, F. Jülicher, K. Kruse, and J. Prost. Hydrodynamic theory for multi-component active polar gels. *New Journal of Physics*, 9, 11 2007.
- [20] A. C. Callan-Jones and F. Jülicher. Hydrodynamics of active permeating gels. *New Journal of Physics*, 13, 9 2011.
- [21] A. C. Callan-Jones and R. Voituriez. Active gel model of amoeboid cell motility. *New Journal of Physics*, 15, 2 2013.
- [22] H. Pleiner, D. Svanšek, and H. R. Brand. Active polar two-fluid macroscopic dynamics. *European Physical Journal E*, 36, 11 2013.
- [23] Harald Pleiner, Daniel Svanšek, and Helmut R. Brand. Hydrodynamics of active polar systems in

- a (visco)elastic background. *Rheologica Acta*, 55:857–870, 10 2016.
- [24] Ananyo Maitra and Sriram Ramaswamy. Oriented active solids. *Physical Review Letters*, 12 2018.
- [25] Ram M. Adar and Jean François Joanny. Permeation instabilities in active polar gels. *Physical Review Letters*, 127, 10 2021.
- [26] Mark Warner and Eugene Michael Terentjev. *Liquid crystal elastomers*, volume 120. Oxford university press, 2007.
- [27] E. J. Hemingway, A. Maitra, S. Banerjee, M. C. Marchetti, S. Ramaswamy, S. M. Fielding, and M. E. Cates. Active viscoelastic matter: From bacterial drag reduction to turbulent solids. *Physical Review Letters*, 114, 3 2015.
- [28] E. J. Hemingway, M. E. Cates, and S. M. Fielding. Viscoelastic and elastomeric active matter: Linear instability and nonlinear dynamics. *Physical Review E*, 93, 3 2016.
- [29] K. Kruse, J. F. Joanny, F. Jülicher, J. Prost, and K. Sekimoto. Generic theory of active polar gels: A paradigm for cytoskeletal dynamics. *European Physical Journal E*, 16:5–16, 1 2005.
- [30] R. Voituriez, J. F. Joanny, and J. Prost. Generic phase diagram of active polar films. *Physical Review Letters*, 96, 1 2006.
- [31] Michael E. Cates and Elsen Tjhung. Theories of binary fluid mixtures: From phase-separation kinetics to active emulsions. *Journal of Fluid Mechanics*, 836:P1, 2 2018.
- [32] J. Prost, F. Jülicher, and J. F. Joanny. Active gel physics. *Nature Physics*, 11:111–117, 1 2015.
- [33] Markus Basan, Thomas Risler, Jean François Joanny, Xavier Sastre-Garau, and Jacques Prost. Homeostatic competition drives tumor growth and metastasis nucleation. *HFSP Journal*, 3:265–272, 8 2009.
- [34] Jonas Ranft, Markus Basan, Jens Elgeti, Jean François Joanny, Jacques Prost, and Frank Jülicher. Fluidization of tissues by cell division and apoptosis. *Proceedings of the National Academy of Sciences of the United States of America*, 107:20863–20868, 12 2010.
- [35] Rumi De, Assaf Zemel, and Samuel A. Safran. Dynamics of cell orientation. *Nature Physics*, 3:655–659, 2007.
- [36] Toyochi Tanaka and David J. Fillmore. Kinetics of swelling of gels. *The Journal of Chemical Physics*, 70:1214–1218, 1979.
- [37] Ilya Levental, Penelope C. Georges, and Paul A. Janmey. Soft biological materials and their impact on cell function. *Soft Matter*, 3:299–306, 2007.
- [38] Arja Ray, Rachel K. Morford, Nima Ghaderi, David J. Odde, and Paolo P. Provenzano. Dynamics of 3d carcinoma cell invasion into aligned collagen. *Integrative Biology (United Kingdom)*, 10:100–112, 2 2018.
- [39] Lakshmi Balasubramaniam, Amin Doostmohammadi, Thuan Beng Saw, Gautham Hari Narayana Sankara Narayana, Romain Mueller, Tien Dang, Minnah Thomas, Shafali Gupta, Surabhi Sonam, Alpha S. Yap, Yusuke Toyama, René Marc Mège, Julia M. Yeomans, and Benoît Ladoux. Investigating the nature of active forces in tissues reveals how contractile cells can form extensile monolayers. *Nature Materials*, 20:1156–1166, 8 2021.
- [40] G. Duclos, C. Blanch-Mercader, V. Yashunsky, G. Salbreux, J. F. Joanny, J. Prost, and P. Silberzan. Spontaneous shear flow in confined cellular nematics. *Nature Physics*, 14:728–732, 7 2018.
- [41] D Blankshtein and R M Hornreich. Theory of phase transitions and modulated structures in ferroelectrics. *PHYSICAL REVIEW B*, 32.
- [42] George A Hinshaw, Rolfe G Petschek, and Robert A Pelcovits. Modulated phases in thin ferroelectric liquid-crystal films. *Physical Review Letters*, 60, 1988.
- [43] M. E. Cates, D. Marenduzzo, I. Pagonabarraga, and J. Tailleur. Arrested phase separation in reproducing bacteria creates a generic route to pattern formation. *Proceedings of the National Academy of Sciences*, 107(26):11715–11720, 2010.
- [44] C. Blanch-Mercader, R. Vincent, E. Bazellères, X. Serra-Picamal, X. Trepast, and J. Casademunt. Effective viscosity and dynamics of spreading epithelia: a solvable model. *Soft Matter*, 13:1235–1243, 2017.

- [45] M. C. Marchetti, J. F. Joanny, S. Ramaswamy, T. B. Liverpool, J. Prost, Madan Rao, and R. Aditi Simha. Hydrodynamics of soft active matter. *Reviews of Modern Physics*, 85:1143–1189, 7 2013.